DYNAMIC SPECTRAL CHARACTERISTICS OF THERMAL MODELS FOR SOLAR HARD X-RAY BURSTS

JOHN C. BROWN and IAN J. D. CRAIG*
Department of Astronomy, University of Glasgow, Glasgow, G12 8QQ, Scotland

and

JUDITH T. KARPEN**
Code 684, Nasa Goddard Space Flight Center, Greenbelt, Md. 20771, U.S.A.

(Received 26 July; in revised form 30 October, 1979)

Abstract. The dynamic spectral characteristics of the thermal model for solar hard X-ray bursts recently proposed by Brown *et al.* (1979) (BMS) are investigated. It is pointed out that this model, in which a single source is heated impulsively and cooled by anomalous conduction across an ion-acoustic turbulent thermal front, predicts that the total source emission measure should rise as the temperature falls. This prediction, which is common to all conductively cooled single-source models, is contrary to observations of many simple spike bursts. It is proposed, therefore, that the hard X-ray source may consist of a distribution of many small impulsively-heated kernels, each cooled by anomalous conduction, with lifetimes shorter than current burst data temporal resolution. In this case the dynamic spectra of bursts are governed by the dynamic evolution of the kernel production process, such as magnetic-field dissipation in the tearing mode. An integral equation is formulated, the solution of which yields information on this kernel production process, from dynamic burst spectra, for any kernel model.

With a BMS-type kernel model in one-dimensional form, the derived instantaneous spectra are limited in hardness to spectral indices $\gamma \geq 4$ for any kernel production process, due to the nature of the conductive cooling. Ion-acoustic conductive cooling in three dimensions, however, increases the limiting spectral hardness to $\gamma \geq 3$. Other forms of anomalous conduction yield similar results but could permit bursts as hard as $\gamma \simeq 2$, consistent with the hardest observed.

The contribution to the X-ray spectrum from the escaping tail of high-energy kernel electrons in the BMS model is calculated in various limits. If this tail dissipates purely collisionally, for example, its thick-target bremsstrahlung can significantly modify the kernel spectrum at the high-energy end. The energetics of this dynamic dissipation model for thermal hard X-ray bursts also are briefly discussed.

1. Introduction

A thermal bremsstrahlung interpretation for solar hard X-ray bursts (≥ 10 keV) was first proposed by Chubb (1970) and, on a more quantitative basis, by Brown (1974). It has also been invoked by Colgate (1978). Kahler (1975; cf. 1971a, b) summarized the problems of this interpretation, the most severe of which are related to the very large temperature gradients implied by the high temperatures involved ($\geq 10^8$ K). These steep gradients would cause the source to cool by classical conduction in a second or less; furthermore, the temperature scale length l_T would be shorter than a collisional mean free path l_c so that the electrons could not relax collisionally to a

* Now at: Department of Mathematics, University of Waikato, Hamilton, New Zealand.
** Astronomy Program, University of Maryland.

Solar Physics **67** (1980) 143–162. 0038-0938/80/0671-0143$03.00.

local Maxwellian distribution. Both factors tend to negate the prime advantage of the thermal model, its efficiency as an X-ray source, by increasing the source electron energy-loss rate much above its minimum (pure radiative) value. Recently, however, Brown *et al.* (1979) – hereafter BMS – have shown how these difficulties might be overcome in realistic flare situations (cf. also Smith and Lilliequist, 1979). Assuming that the plasma heating process produces much higher electron temperatures (T_e) than proton temperatures (T_p), BMS note that the condition $l_T \ll l_c$ results initially in free expansion of the hot electrons into the cool surroundings, thus driving a reverse current which is unstable to generation of ion-sound waves. The resulting ion-sound turbulent boundaries and associated electric field bottle up the hot electron flux and maintain a near-Maxwellian electron distribution (apart from an escaping high-energy tail) by providing a collisionless scattering process. Conductive cooling times are thus anomalously increased, by a factor which depends on the level of turbulence attained and which could be of order 10^4 or greater. According to the approximate BMS analytic treatment, the anomalous conduction front remains near marginal stability, thus propagating heat into the cool plasma at the ion-sound speed $v_s = \sqrt{T_e/m_p}$. (Temperatures are in energy units throughout.) Cooling times are increased over the classical (flux-limited collisional conduction) values by the factor $v_e/v_s = m_p/m_e = 43$ (where $v_e = \sqrt{T_e/m_e}$), comparable to the results of the detailed computations of Smith and Lilliequist (1979). Such an increase renders the BMS burst model viable in terms of typical spike-burst peak emission measures and durations (cf. Crannell *et al.*, 1978) for reasonable source dimensions ($L \lesssim 10^3$ km), and compatible with interplanetary electron data for source densities $n_e \lesssim 5 \times 10^{11}$ cm^{-3} (cf. BMS). In its original presentation, however, the BMS dissipative thermal model was not tested observationally in terms of detailed behaviour such as X-ray spectral evolution and polarisation (cf. adiabatic thermal model by Crannell *et al.* (1978) and Mätzler *et al.* (1978)). Emslie and Brown (1980) have shown the BMS model to be compatible with the very limited data available on burst polarisation and directivity.

In this paper we investigate the dynamic spectral characteristics of the model and, in particular, show (Section 2) that a conductively cooled single kernel is incompatible with the observed spectral decay of even a simple spike event (Crannell *et al.*, 1978). We then show (Section 3) that the dissipative thermal model is consistent with the data if the source comprises not a single BMS-type kernel but rather an assembly of numerous, small, dissipative kernels, each very short-lived, which are continuously produced throughout the spike burst. Such a continuously varying, inhomogeneous thermal structure is indeed what one would expect from primary dissipation in the tearing mode, such as in Spicer's (1976, 1977) unstable arch model with its islands of magnetic dissipation, and is essential to the interpretation of 'multiple spike' events (cf. Hoyng *et al.*, 1976; Karpen *et al.*, 1979). Spatially it is also analogous to the inhomogeneous structures which must be invoked to explain both burst evolution and quiescent sources in soft X-rays (e.g. Craig *et al.*, 1978).

2. Dynamic Spectra of Hard X-Ray Bursts and the BMS Model

Kane and Anderson (1970) were the first to show that the rise and decay times of hard X-ray bursts both decrease with increasing photon energy, so that the burst spectrum is hardest at the time of peak flux. While larger events do not necessarily exhibit this relationship (cf. Hoyng *et al.*, 1976), this behaviour has been amply confirmed, by independent experiments, for events which are either small (e.g. Datlowe *et al.*, 1974a; Elcan, 1978) or have simple time structure (e.g. Crannell *et al.*, 1978). Since spectra of most events are observed only over about one decade in photon energy ε, they can be fitted by a variety of two-parameter functions (cf. Brown, 1978). The most commonly used are the ('non-thermal') power-law, $I \sim a\varepsilon^{-\gamma}$, and the ('thermal') exponential, $I \sim b\varepsilon^{-1} \exp(-\varepsilon/T)$, sometimes corrected for Gaunt factor and albedo (cf. Crannell *et al.*, 1978). These two-parameter representations of dynamic spectral data can be used to plot the burst time (t) evolution conveniently as a locus described in the plane of the parameters, i.e. $a(t)$ versus $\gamma(t)$ or $b(t)$ versus $T(t)$. The former is equivalent to a plot of thick-target electron flux versus spectral index (cf. Hoyng *et al.*, 1976) and the latter to a plot of isothermal emission measure EM versus $T \equiv T_e$ (cf. Mätzler *et al.*, 1978). A typical plot of the latter type (Mätzler *et al.*, 1978, Figures 7 and 10 – see Figure 1) for a single spike event exhibits a monotonic rise and fall of EM as T rises and falls respectively; this is a graphical representation of the basic findings of Kane and Anderson (1970). Note that this decline of $EM(t)$ with $T(t)$ is precisely opposite to the pattern observed in the soft X-ray range (e.g., Zaumen and Acton, 1974; Datlowe *et al.*, 1974b). (Elcan (1978) reports an increase of EM with T in some of his 'hard' X-ray events which may indicate a different class of event or merely that he is really observing the soft component since the observed energies are rather low.)

If a single hard X-ray spike is produced by the impulsive heating of a single plasma kernel, we expect the spectral properties of the burst rise to be dominated by the heating mechanism, while the decay is controlled mainly by the cooling process. In the BMS model the heating mechanism is assumed to be dissipative (not adiabatic), localised and impulsive, and resulting in $T_e \gg T_p$; Smith and Lilliequist (1979) assume an empirical heat pulse form. Magnetic-field annihilation in a magnetic island of the tearing mode (Fürth *et al.*, 1963; Drake and Lee, 1977; Spicer, 1976, 1977) is recognized as one possibility. We will return to the question of heating processes shortly but for the moment we consider only the decay phase. Following BMS, we take this to be conductive and at constant density n_0, since the convection time L/v_p (where $v_p = \sqrt{T_p/m_p}$) greatly exceeds the anomalous conduction time L/v_s for $T_e \gg T_p$ (cf. later discussion). Since the radiative losses are energetically negligible, the effect of conduction is simply to spread the total initial thermal energy (impulsively deposited) through an ever-increasing volume $V(t)$ (cf. Zaumen and Acton, 1974); that is,

$$n_0 V(t) T(t) = n_0 V_0 T_0 . \tag{1}$$

Thus the emission measure $EM = n_0^2 V$ is related to T by

$$EM(t)T(t) = EM_0 T_0 , \tag{2}$$

which directly contradicts the observed correlation of $EM(t)$ and $T(t)$. Note that this argument applies irrespective of the particular rate at which $T(t)$ falls, and so is not specific to the BMS model but applies to any conductive case. Furthermore, the conclusion is unchanged by continuing energy input $P(t)$ to the volume after burst peak, since this merely adds a positive term $(\int_t P \, dt)$ to the right of (1) and can never result in $EM(t)$ decreasing as $T(t)$ decreases.

There are two possible ways out of this discrepancy. One is to invoke a decrease of density n as T falls and V rises such that $EM = n^2 V$ declines. Such rarefaction could arise by hydrodynamic expansion, but only on a time scale long compared to the electron conduction time if $T_e \gg T_p$ (cf. Smith and Lilliequist, 1979, and discussion in Section 5), or be driven by adiabatic compression and rarefaction of a kernel under the action of magnetic-field changes (Crannell *et al.*, 1978; Mätzler *et al.*, 1978). Such adiabatic heating requires strong fields and rather special geometry for the heating and cooling to occur sufficiently quickly that conduction along the field lines does not violate the adiabatic condition. In addition, the plasma must be preheated substantially to achieve high enough peak temperatures without demanding unreasonably large field-compression ratios.

The second possibility is to adhere to a kernel model with localized impulsive dissipation, such as BMS, but to suppose that there are many small kernels produced continuously throughout the burst, each much shorter lived than the burst duration even for a simple spike burst event. Such a description actually is (qualitatively) in much better agreement with the physics of tearing-mode dissipation than is a single hot kernel. The dynamic spectral evolution of the burst as a whole will then, in general, be a convolution of the spectral behaviour of all hot kernels present in the entire source at each instant, and will be governed by the distribution of kernel production properties in both space and time.

An interesting limiting case to consider is that in which each kernel has a lifetime much shorter than the instrumental resolution. Then the total instantaneous source emission rate is given approximately by the typical peak emission rate for one kernel, governed by the peak kernel EM and T, times the typical kernel lifetime, governed by its size and peak temperature (cf. BMS), times the rate of production of kernels at that instant. This situation is closely analogous to that of non-thermal burst models which invoke continuous injection of electrons into a thick target, where energy loss occurs in a time short compared to resolution (cf. Acton, 1968; Arnoldy *et al.*, 1968; and Brown, 1971, for example). The observed behaviour of EM versus T is then to be interpreted as a relation between the instantaneous mean temperature of the kernels present in the source and their instantaneous total effective emission measure. The latter will equal approximately the instantaneous rate of production of emission measure in all the kernels times the mean kernel lifetime at that instant. Specifically, the $EM(T)$ path of Mätzler *et al.* (1978) – Figure 1 – would imply that as

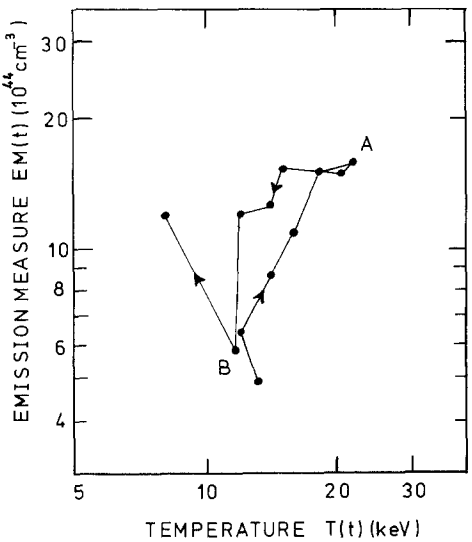

Fig. 1. Spectral evolution of the hard X-ray burst of March 1, 1969 at $22^h\,53^m$ UT shown in terms of the locus described in the plane of the instantaneous best fit temperature $T(t)$ and total emission measure $EM(t)$ for an isothermal model (from Mätzler *et al.*, 1978). Note particularly the decline of $EM(t)$ with $T(t)$ in the decay AB.

an arch (for example) went unstable, hot kernels would be produced at a steadily increasing rate with steadily increasing mean temperature until burst peak, and at a declining rate and decreasing mean temperature thereafter. In multiple-spike events the whole process would be repeated during each successive peak, possibly corresponding to spread of the instability through the inhomogeneous magnetic arch structure. Such a description seems physically plausible but to see whether it is consistent with the observations in detail, however, we must evaluate the kernel spectral properties more closely than in terms of a mean emission measure, temperature and lifetime. In particular, since each kernel emits throughout its decay the spectral contribution will be softer (steeper) than that at peak temperature, and we can qualitatively expect steeper spectra from the ensemble of kernels than from a single isothermal kernel. We now investigate in detail the spectral properties for this model of dynamic kernel superposition in the case where the cooling of each kernel is as described by BMS.

3. Spectral Properties of Thermal Model with Continuous Production of Short-Lived Kernels

3.1. General formulation

Consider first an arbitrary kernel, K, heated and cooled in a total time t_K ($\ll$data resolution), with an emission measure $EM_K(t)$ and a temperature $T_K(t)$ (in energy

units) at instant t within t_K. During its lifetime this kernel will produce a pulse of X-rays at the Earth with spectrum:

$$\mathcal{I}_K \text{ (photons cm}^{-2} \text{ per unit } \varepsilon) = \frac{C}{\varepsilon} \int_{t_K} EM_K(t) \frac{e^{-\varepsilon/T_K(t)}}{T_K^{1/2}(t)} \mathrm{d}t, \tag{3}$$

where $C = 2.4 \times 10^{-42}$ for ε and T_K in keV and the Gaunt factor is taken as unity. The values of $T_K(t)$, $EM_K(t)$ and t_K depend on the heating and cooling mechanisms and on initial characteristics of the kernel such as density, volume, and magnetic-field strength, all of which we represent by a parameter (or set of parameters) K. Thus, when we next consider time scales long compared to t_K we will have an instantaneous rate of production of kernels $Q_K(t)$ per unit range of parameter(s) K and a resulting photon flux spectrum $I(\varepsilon, t)$ (photons cm^{-2} s^{-1} per unit ε) at the Earth:

$$I(\varepsilon, t) = \int_K Q_K(t) \mathcal{I}_K(\varepsilon) \, \mathrm{d}K. \tag{4}$$

More generally, if t_K is not small compared to the instrumental resolution or to the time scale for variations of Q_K then (4) must be generalized to a convolution of emissions from kernels formed at all preceding times. We now see that the qualitative discussion at the end of Section 2 is equivalent to replacing (3) by the approximation

$$\mathcal{I}_K(\varepsilon) = \frac{C}{\varepsilon} \overline{EM}_K \frac{e^{-\varepsilon/\bar{T}_K}}{\bar{T}_K^{1/2}} \bar{t}_K. \tag{5}$$

According to Equation (4), therefore,

$$I(\varepsilon, t) = \frac{C}{\varepsilon} \int_K \{Q_K(t) \overline{EM}_K(t) \bar{t}_K(t)\} \frac{e^{-\varepsilon/\bar{T}_K}}{\bar{T}_K^{1/2}} \, \mathrm{d}K, \tag{6}$$

where the bracketed term is an effective instantaneous emission measure per unit K for the entire source.

This discussion so far is quite general in that, given *any* model of a short-lived hot kernel, we can evaluate $\mathcal{I}_K$ from (3) and hence relate $I(\varepsilon, t)$ to $Q_K(t)$ via (4). We will first consider in detail the particular $\mathcal{I}_K(\varepsilon)$ obtained in the basic BMS model, to test the predictions of that model and to illustrate the above analysis in a particular case.

3.2. Analysis for one-dimensional BMS-type kernel

To obtain $\mathcal{I}_K(\varepsilon)$ we must consider $EM_K(t)$ and $T_K(t)$ in both the kernel heating and cooling phases. Available heating mechanisms are little understood as yet and so we merely mention some possible candidates. Anomalous local joule heating in a

magnetic island of the tearing mode has been proposed as the primary flare energy release mechanism (Fürth *et al.*, 1963; Drake and Lee, 1977; Spicer, 1976, 1977). According to D. S. Spicer (personal communication) this process can result in local heating of electrons in a few plasma periods up to the required temperatures $\gtrsim 10^8$ K. A second possibility is electron heating in regions of ion-sound turbulence. In this case (Duijveman and Hoyng, 1980) the heating time and peak temperatures achieved are very sensitive to the several parameters involved, but for plausible values could produce electron heating to temperatures $\gtrsim 10^8$ K in about 10^{-2} to 10^{-1} s. In both situations the heated regions are localized sites within the flare energy-release volume and, for plausible parameter values, may have cooling times due to anomalous thermal conduction (as in the BMS model) in the range 10^{-1} to 1 s for kernels with a plausible size of say $\simeq 100$ km. (cf. BMS; and also Brown and Nakagawa, 1978). These rough estimates show that the lifetimes of individual kernels may indeed be below current hard X-ray instrumental time resolution as suggested above. Furthermore, the brevity of the kernel heating times as compared to their cooling times indicates that most of the X-ray emission from a single kernel will occur during its decay phase. We therefore adopt the idealisation that $\mathcal{I}_K$ can be adequately determined by performing the integral (3) over the kernel cooling phase alone.

A one-dimensional kernel (cf. Section 3.4) cooled by anomalous conduction (cf. Section 3.5) in the fashion described by BMS can be characterized by the following parameters: the constant density n_0, constant cross-sectional area A_0, peak electron temperature T_0 and initial length L_0. The kernel length L extends at a speed $v_s = (T/m_p)^{1/2}$ such that $L(t)T(t)$ remains constant (cf. Section 2), that is

$$\frac{dL}{dt} = \left(\frac{T}{m_p}\right)^{1/2} \quad \text{and} \quad L\frac{dT}{dt} + T\frac{dL}{dt} = 0\,, \tag{7a}$$

whence

$$\frac{dT}{dt} = -\frac{T}{L}\frac{dL}{dt} = -\frac{T^{5/2}}{L_0 T_0 m_p^{1/2}}\,, \tag{7b}$$

and so

$$\frac{T_0}{T(t)} = \frac{L(t)}{L_0} = \frac{EM(t)}{EM_0} = \left(1 + \frac{t}{t_0}\right)^{2/3}\,, \tag{7}$$

where $t_0 = \frac{2}{3}L_0/(T_0/m_p)^{1/2}$ is the characteristic kernel cooling time and $EM(t) = n_0^2 A_0 L(t)$. Note that for the present we treat the BMS kernel as having a Maxwellian distribution of electrons at temperature T. We thus neglect the fact that the tail of the distribution at $v > 2.6v_e$ escapes (cf. BMS), on the grounds that the number of electrons in the tail is too small to contribute much bremsstrahlung except at high

photon energies. We return to the effects of this assumption in Section 4. Equations (3) and (7) yield

$$\mathcal{I}(\varepsilon) = C\frac{EM_0}{\varepsilon T_0^{1/2}} \int_{t=0}^{\infty} \left(1+\frac{t}{t_0}\right) \exp\left\{-\frac{\varepsilon}{T}\left(1+\frac{t}{t_0}\right)^{2/3}\right\} \mathrm{d}t =$$

$$= \tfrac{3}{2} CEM_0 t_0 \frac{T_0^{5/2}}{\varepsilon^4} e^{-\varepsilon/T_0}\left\{2+\frac{2\varepsilon}{T_0}+\frac{\varepsilon^2}{T_0^2}\right\}. \tag{8}$$

We have formally extended (3) over an infinite t range though in practice the main contribution is made within $t_K \simeq t_0$, much less than time scales on which deviations from (7) occur due to hydrodynamic and other effects.

Such kernels can be described by the set of parameters $K = (EM_0; T_0; t_0)$ and (6) can be written

$$I(\varepsilon, t) = \frac{3}{2}\frac{C}{\varepsilon^4} \int_{T_0} \int_{EM_0} \int_{t_0} [Q(T_0, EM_0, t_0) EM_0 t_0] T_0^{5/2} e^{-\varepsilon/T_0} \times$$

$$\times \left\{2+\frac{2\varepsilon}{T_0}+\frac{\varepsilon^2}{T_0^2}\right\} \mathrm{d}T_0 \, \mathrm{d}EM_0 \, \mathrm{d}t_0 , \tag{9}$$

where Q is the kernel production rate per second per unit range of emission measure, temperature, and lifetime. Clearly, given $I(\varepsilon, t)$, solution of integral Equation (9) can only yield an average value of the function in square brackets (over EM_0 and t_0), viz.

$$\xi_{\mathrm{eff}}(T_0, t) = \int_{EM_0} \int_{t_0} [Q(T_0, EM_0, t_0) t_0] \, EM_0 \, \mathrm{d}EM_0 \, \mathrm{d}t_0 , \tag{10}$$

which can be seen to be the effective instantaneous emission measure differential in temperature. This quantity can also be interpreted as a mean kernel production rate per unit T_0 weighted relative to their emission measures and lifetimes; thus the largest and coolest kernels have greatest weight. The problem of interest is then the solution of

$$\int_{T_0=0}^{\infty} \xi_{\mathrm{eff}}(T_0) T_0^{5/2} e^{-\varepsilon/T_0}\left\{2+\frac{2\varepsilon}{T_0}+\frac{\varepsilon^2}{T_0^2}\right\} \mathrm{d}T_0 = \frac{2}{3C}\varepsilon^4 I(\varepsilon) \tag{11}$$

at each instant; note that the t dependence in ξ_{eff} and I have been dropped accordingly. The kernel of this integral equation now contains the additional factor $\varepsilon^{-3}\{2+2\varepsilon/T_0+\varepsilon^2/T_0^2\}$ compared to the result (6) of our earlier simplified discussion, due to the inclusion of the correct spectral decay factor for each BMS kernel.

Equation (11) may be handled in the usual manner, either by inversion to find $\xi_{\mathrm{eff}}(T_0)$ from an observed $I(\varepsilon)$ or by fitting predicted forms of $I(\varepsilon)$ from model forms of

$\xi_{\text{eff}}(T_0)$. It is important, however, to recognize the problems of instability in the former approach and of non-uniqueness in the latter (cf. Craig and Brown, 1976). Analytic inversion of (11) may be cast into convenient form by defining

$$\begin{aligned} \tau &= 1/T_0\,, \\ G(\tau) &= \xi_{\text{eff}}(T_0) T_0^{9/2}\,, \\ H(\varepsilon) &= \frac{2}{3C} I(\varepsilon)\varepsilon^4\,, \end{aligned} \tag{12}$$

whence (11) becomes

$$\int_0^\infty G(\tau)\{2+2\varepsilon\tau+\varepsilon^2\tau^2\}\, e^{-\varepsilon\tau}\, \mathrm{d}\tau = H(\varepsilon)\,. \tag{13}$$

Introducing the Laplace transform $\tilde{G}$ of G,

$$\tilde{G}(\varepsilon) = \mathfrak{L}\{G(\tau);\varepsilon\} = \int_0^\infty G(\tau)\, e^{-\varepsilon\tau}\, \mathrm{d}\tau\,, \tag{14}$$

yields a more concise form for (13):

$$\varepsilon^2 \frac{\mathrm{d}}{\mathrm{d}\varepsilon}\left[\varepsilon^2 \frac{\mathrm{d}}{\mathrm{d}\varepsilon}\left(\frac{\tilde{G}}{\varepsilon^2}\right)\right] = H(\varepsilon)\,, \tag{15}$$

where it is understood that, in order to maintain exact equivalence to (13), the constants of integration must vanish. With this convention we obtain the formal inversion formula

$$G(\tau) = \mathfrak{L}^{-1}\left\{\varepsilon^2 \int_\varepsilon^\infty \frac{dy}{y^2} \int_y^\infty \frac{H(x)}{x^2}\,\mathrm{d}x;\tau\right\} \tag{16}$$

or, in terms of the original variables

$$\xi_{\text{eff}}(T_0) = \frac{2}{3C}\, T_0^{-9/2}\, \mathfrak{L}^{-1}\left\{\varepsilon^2 \int_\varepsilon^\infty \frac{\mathrm{d}y}{y^2} \int_y^\infty x^2 I(x)\,\mathrm{d}x;\frac{1}{T_0}\right\}. \tag{17}$$

3.3. Application to observations

Inversion formula (17) immediately provides insight into the forms of spectra possible from a dynamic BMS kernel model in the one-dimensional (1-D) case. For example, the simple spike bursts studied by Crannell *et al.* (1978) (cf. also Elcan, 1978) were found to have spectra consistent with that from a single, isothermal, bremsstrahlung source; that is, their instantaneous spectra can be approximated by

$$I(\varepsilon) = \frac{a}{\varepsilon}\, e^{-\varepsilon/\varepsilon_0}\,, \tag{18}$$

neglecting albedo corrections and with unit Gaunt factor. If this were the true spectrum over all ε, then a kernel distribution would be required, according to (17), with

$$\xi_{\text{eff}}(T_0) = \frac{2a}{3C}\,\varepsilon_0^2\,T_0^{-9/2}\,\mathfrak{L}^{-1}\left\{\varepsilon\,e^{-\varepsilon/\varepsilon_0};\frac{1}{T_0}\right\}. \tag{19}$$

No such inverse Laplace transform exists for any wholly positive function $\xi_{\text{eff}}(T_i)$, however, since $G(\tau)>0$ in (15) leads to monotonic decrease of $\tilde{G}(\varepsilon)$ with increasing ε. This result indicates that the model is only capable of yielding a limited range of burst spectra, those for which positive solutions of (17) exist.

On course in practice we are not concerned with spectra of exact analytic forms like (18), but rather with the consistency of models with noisy spectral data over a finite energy range. Insight into this problem may be gained by considering some simple illustrative examples for $\xi_{\text{eff}}(T_0)$ in (11) and evaluating $I(\varepsilon)$. The simplest conceivable case is that in which kernels are being produced, at any instant, only over a narrow range of temperature $T_0 \simeq T_1$ and with initial sizes and lifetimes dependent only on T_1. Then

$$\xi_{\text{eff}}(T_0) = \xi_1\delta(T_0 - T_1)\,, \tag{20}$$

where δ is the delta-function (defined such that $\int \delta(T)\,\mathrm{d}T = 1$). The resulting spectrum is, by (11),

$$I_1(\varepsilon) = \frac{3}{2}\,C\frac{\xi_1}{T_1^{3/2}}\,e^{-\varepsilon/T_1}\left(\frac{T_1}{\varepsilon}\right)^4\left\{2+\frac{2\varepsilon}{T_1}+\frac{\varepsilon^2}{T_1^2}\right\}. \tag{21}$$

Another possibility is that ξ_{eff} is constant up to some maximum $T_0 = T_2$ and zero above, i.e.,

$$\xi_{\text{eff}} = \begin{cases} \xi_2/T_2, & T_0 \le T_2\,, \\ 0, & T_0 > T_2\,, \end{cases} \tag{22}$$

for which

$$I(\varepsilon) = \frac{3}{8}\,C\frac{\xi_2}{T_2^{3/2}}\,e^{-\varepsilon/T_2}\left(\frac{T_2}{\varepsilon}\right)^4\left\{2+\frac{2\varepsilon}{T_2}+\left(\frac{\varepsilon}{T_2}\right)^2-\left(\frac{\varepsilon}{T_2}\right)^3\left[1-f\left(\frac{\varepsilon}{T_2}\right)\right]\right\}, \tag{23}$$

where $f(x) = x\,e^x E_1(x) \simeq 0.545 + 0.405\,\log_e x$ (E_1 = first exponential integral). We have found spectral forms essentially similar to (21) and (23) for all models of $\xi_{\text{eff}}(T_0)$ involving a finite maximum T_0, apart from variations in the { } bracketed factor. When $\xi_{\text{eff}}(T_0)$ is allowed to extend to arbitrarily high T_0 in the power-law form

$$\xi_{\text{eff}}(T_0) = \frac{\xi_3}{T_3}\left(\frac{T_0}{T_3}\right)^{-a}, \tag{24}$$

the burst spectrum becomes

$$I_3(\varepsilon) = \tfrac{3}{2}C(\alpha-\tfrac{5}{2})(\alpha-\tfrac{3}{2})\Gamma(\alpha-\tfrac{7}{2})\,\frac{\xi_3}{T_3^{3/2}}\left(\frac{\varepsilon}{T_3}\right)^{-\alpha-1/2}, \tag{25}$$

where Γ is the gamma function.

Spectra (21), (23), and (25) exhibit the following important properties: Those with finite maximum temperature T_M in ξ_{eff} behave like the power-law $I(\varepsilon) \sim \varepsilon^{-4}$ at $\varepsilon \ll T_M$ and like $I(\varepsilon) \sim \varepsilon^{-\gamma} e^{-\varepsilon/T_M}$ with $\gamma \simeq 2$ to 3 at $\varepsilon \gg T_M$; thus, these spectra are never flatter than ε^{-4}. Power-law spectrum (25) with $T \to \infty$, however, can likewise never be flatter than ε^{-4} for any physically plausible value ξ_3 since, mathematically, the gamma function only exists for $\alpha > \frac{7}{2}$. These lower limits to the spectral steepness produced by the dynamic BMS kernel model arise because no convolution with a physically possible $\xi_{\text{eff}}(T_0)$ can overcome the intrinsic steepness of the spectrum $\mathcal{J}(\varepsilon)$ of the individual bremsstrahlung kernel arising from its cooling properties.

According to Kane (1974), about 70% of small impulsive bursts have spectra with $\gamma \gtrsim 4$, for the power-law fit $I(\varepsilon) \sim \varepsilon^{-\gamma}$. Thus we conclude that the dynamic BMS kernel model in one dimension is capable of producing spectra compatible with the majority of impulsive bursts. As a specific example, we have best fit our model spectrum (21) near the peak of the OSO-5 single spike burst of March 1, 1969 at UT $22^{\text{h}}\,53^{\text{m}}\,12^{\text{s}}$ (Crannell *et al.*, 1978) shown in Figure 1, and obtained an acceptable fit, within the data noise, for the parameters $\xi_1 \simeq 4.7 \times 10^{43}\ \text{cm}^{-3}$ and $T_1 \simeq 45$ keV. As expected, this temperature is somewhat higher than the 25 keV found by Crannell *et al.* (1978) under the assumption of a single isothermal source. An acceptable fit is also obtained for models (23) and (25) with comparable temperatures and emission measures. Ambiquity arises in interpreting this ξ_1 physically since no direct information is available on the initial size L_0 and density n_0 of each kernel. Treating these as free parameters to be determined from other data or from kernel heating models, we see that the total volume of *all* the kernels *instantaneously* present is $V_I = \xi_1/n_0^2 \simeq 6 \times 10^{21}\ \text{cm}^3/(n_0/10^{11})^2$, where n_0 is in units of cm^{-3}. Each of these kernels has a lifetime $t_0 \simeq L_0/(T_1/m_p)^{1/2} \simeq 5 \times 10^{-2}\ (L_0/100)\ \text{s}$ and a volume $\Delta V \lesssim L_0^3\ \text{km}^3$, (depending on the transverse geometry), where L_0 is in units of km. Thus, the number of kernels instantaneously present is $N_I = V_I/\Delta V \gtrsim 6/[(L_0/100)^3(n_0/10^{11})]$; the kernel production rate is $N_I/t_0 \simeq 100/[(L_0/100)^4(n_0/10^{11})]\ \text{s}^{-1}$; and the emission measure production rate is $\xi_1/t_0 \simeq 10^{45}/[(L_0/100)]\ \text{cm}^{-3}\ \text{s}^{-1}$. This event had a total e-folding duration $t_x \simeq 20\ \text{s}$ so the total number of kernels produced during the event is $N_T \simeq N_I t_x/t_0 \simeq 2 \times 10^3/[(L_0/100)^4(n_0/10^{11})]$. The total emission measure produced is $\xi_T = \xi_I t_x/t_0 = 2 \times 10^{46}/[(L_0/100)]\ \text{cm}^{-3}$, and the total volume $V_{\text{tot}} = V_I t_x/t_0 = 2 \times 10^{24}\ \text{cm}^3/[(n_0/10^{11})^2(L_0/100)]$.

On the other hand, a significant fraction of impulsive bursts have spectra with $\gamma \lesssim 4$, and it is clear that the dynamic kernel model with 1-D BMS kernels cannot produce them. Consequently, we consider modifications of the short-lived kernel itself, from its basic form as presented by BMS, which may affect the spectral characteristics of the dynamic kernel model through the kernel cooling properties. Since we have shown that the problem of spectral steepness stems essentially from the spectrum produced by a single kernel, it will suffice to evaluate $\mathcal{J}(\varepsilon)$ for these modified kernel models.

3.4. Spectrum from a three-dimensional BMS-type kernel

The heating produced in a kernel, especially in larger bursts, may be intense enough to produce conductive cooling in 3-D instead of simply along rigid 1-D field lines. We consider here the extreme case of a spherical conduction front of radius $R(t)$ around a region of temperature $T(t)$, again propagating at the ion-sound speed in a plasma of uniform density n_0. For this geometry, Equation (7) is replaced, using a similar derivation, by

$$\frac{EM(t)}{EM_0}=\frac{T_0}{T(t)}=\frac{R^3(t)}{R_0^3}=\left(1+\frac{t}{t_0}\right)^{6/5}, \tag{26}$$

where $t_0=R_0/(T_0/m_p)^{1/2}$. A treatment similar to that of the 1-D case leads to

$$\mathscr{I}(\varepsilon)=\tfrac{5}{6}C\frac{EM_0t_0}{T_0^{3/2}}\left[\frac{T_0}{\varepsilon}\right]^{10/3}\Gamma(\varepsilon/T_0,\tfrac{7}{3}), \tag{27}$$

where

$$\Gamma(a,b)=\int_a^\infty x^{b-1}\,e^{-x}\,\mathrm{d}x \tag{28}$$

is the incomplete gamma function.

This kernel spectrum is hardest at $\varepsilon \ll T_0$, where $\mathscr{I}(\varepsilon)\sim\varepsilon^{-10/3}$ while $\mathscr{I}(\varepsilon)\sim\varepsilon^{-2}\,e^{-\varepsilon/T_0}$ at $\varepsilon \gg T_0$. These spectra are approximately one power harder than the corresponding spectra in the 1-D case because, for a given T_0, a 3-D kernel cools more rapidly than in the 1-D case. A higher proportion of the kernel emission thus originates at high temperatures. Extension of the BMS kernel model to the 3-dimensional case allows substantially harder spectra to be generated in a dynamic kernel situation, the range $\gamma \gtrsim 3$ covering virtually all small impulsive bursts (Kane, 1974).

3.5. Spectrum for more general types of conductively cooled kernels

The BMS treatment is limited to a specialised form of conductive cooling law: an ion-sound turbulent conduction front at marginal stability. Deviation from marginal stability, extension of the wave turbulent region through the entire bremsstrahlung source, (Auer and Smith, 1979) or the presence of other types of wave turbulence all may lead to important changes in the conductive cooling behaviour of kernels. We investigate this possibility parametrically by using the self-similar adiabatic conduction solution for a highly transient and localised heating in a gas with thermal conductivity $\kappa(T)=\kappa_0T^\beta$ (e.g. Zeldovich and Raizer, 1967, p. 657 *et seq.*). For the

1-D case this solution gives

$$\frac{EM(t)}{EM_*} = \frac{T_*}{T(t)} = \left(\frac{t}{t_*}\right)^{1/(\beta+2)}, \tag{29}$$

where EM_*, T_*, and t_* are, respectively, a mean emission measure and temperature during the cooling and a characteristic cooling time. These parameters depend on the kernel density and area, the conductivity parameters κ_0 and β, and on the energy deposition per unit area (or the energy deposition at a point in the 3-D case treated below) but the actual form of this dependence is irrelevant here since it does not affect the kernel spectral distribution. Substituting (29) into (3) yields, for this kernel model,

$$\mathcal{I}(\varepsilon) = \frac{C}{\varepsilon}\frac{EM_*}{T_*^{1/2}} \int_0^\infty \left(\frac{t}{t_*}\right)^{3/[2(\beta+2)]} \exp\left[-\frac{\varepsilon}{T_*}\left(\frac{t}{t_*}\right)^{1/(\beta+2)}\right] dt =$$

$$= C\frac{EM_* t_*}{T_*^{3/2}}(\beta+2)\Gamma(\beta+\tfrac{7}{2})\left(\frac{T_*}{\varepsilon}\right)^{\beta+9/2}. \tag{30}$$

In the 3-D case of the self-similar solution (point heating) the corresponding equations are

$$\frac{EM(t)}{EM_*} = \frac{T_*}{T(t)} = \left(\frac{t}{t_*}\right)^{3/(3\beta+2)} \tag{31}$$

giving

$$\mathcal{I}(\varepsilon) = C\frac{EM_* t_*}{T_*^{3/2}}\frac{(3\beta+2)}{3}\Gamma(\beta+\tfrac{13}{6})\left(\frac{T_*}{\varepsilon}\right)^{\beta+19/6}. \tag{32}$$

The hardness of the spectra (30) and (32), in the 1-D and 3-D cases, depends on the conductivity index β. For classical (collisional) conductivity $\beta = \frac{5}{2}$, the kernel spectra are very steep: $\gamma = 7$ and $\gamma = 5.7$ for the 1-D and 3-D cases respectively. Anomalous conductivity conditions generally result in a reduction of the conductivity index β as well as of κ_0. For instance, though there is no exact equivalence between the evolution of EM and T in the BMS description and any self-similar solution, the self-similar conduction front propagates at the ion-sound speed (as in BMS) for $\beta = -\frac{1}{2}$ and a suitable κ_0. Auer and Smith (1979) also have reported an effective conductivity with $\beta \simeq -\frac{1}{2}$ in one regime of their detailed numerical treatment of the same problem as studied in the approximate BMS treatment. From (30) and (32) we see that a dynamic model with conductivity characterized by $\beta \simeq -\frac{1}{2}$ would yield spectra $\sim\varepsilon^{-4}$ and $\sim\varepsilon^{-2.5}$ in the 1-D and 3-D cases respectively, comparable with the hardest spectra ever observed.

4. The Spectral Contribution of the Maxwellian Tail

Throughout Section 3 the emission from an impulsively heated kernel has been treated as if the kernel electrons had a complete Maxwellian velocity distribution at a single homogeneous temperature. However, BMS pointed out that electrons of $v > (m_p/m_e)^{1/8}\, v_e \simeq 2.6 v_e$, effectively are unscattered by the ion-sound turbulence in the conduction front, and therefore escape. Clearly, this deviation from a strictly Maxwellian electron distribution within each kernel might modify significantly our calculated kernel spectra, particularly at high energies. The dynamics of the tail have not been adequately investigated as yet (cf. Vlahos and Papadapoulos, 1979) so we restrict our analysis to limiting cases. It should be noted that since the tail electrons ($v \gtrsim 2.6 v_e$) are not scattered by the turbulent front, it may be impossible for the tail to form at all unless there is another redistribution process present (cf. Emslie and Brown, 1979). If the tail is formed by the impulsive heating process itself, it will escape at once and deposit its energy elsewhere, emitting bremsstrahlung as it does so. The maximum bremsstrahlung yield of the tail would occur if it descended into the collisionally thick chromosphere and suffered only collisional losses (i.e., thick target case). In practice the tail electrons will also lose energy in the beam relaxation process (Vlahos and Papadapoulos, 1979) and under the action of the electric field driving the reverse current generated by both tail electrons (Ionson, 1978) and the conducting electrons (Smith and Brown, 1979). Thus, by calculating the thick-target emission from an escaping tail we obtain an upper limit to its bremsstrahlung contribution. Note also that if a single kernel were used to describe a simple impulsive event, as proposed by BMS, then any thick-target tail emission should appear as a very brief spike at the start of the burst. In the situation proposed here involving dynamic production of many kernels, however, the thick-target spikes from a single kernel simply would add to the thermal kernel emission, both occurring in times too short to be resolved by present instrumentation.

We have calculated, therefore, the kernel X-ray pulse spectrum $\mathcal{I}(\varepsilon)$ in three cases: (a) when the kernel electron distribution is a complete Maxwellian throughout (as assumed in Section 3); (b) when the distribution is a Maxwellian truncated at $v = 2.6 v_e$, and no tail is present; (c) when the tail is fully formed at peak kernel heating but then escapes at once to emit thick-target bremsstrahlung elsewhere. To make these calculations of thermal and non-thermal bremsstrahlung analytically tractable we have used throughout this section the differential bremsstrahlung cross-section approximation $\sigma(\varepsilon, E) = \sigma_0/\varepsilon E$ (at electron energy E), which is consistent with (3) and sufficient for purposes of *comparison* of the spectra in our three cases, (cf. calculation by Vlahos and Emslie (1979) using Bethe-Heitler cross-section). We also have confined ourselves to the 1-D situation of a kernel with cross-sectional area A_0 and other initial parameters as defined in Section 3.2. Cases (a) and (b) are treated straightforwardly as before and yield (with $R = 1$ AU)

$$\mathcal{I}_a(\varepsilon) = \frac{3}{(2\pi)^{3/2}} \frac{\sigma_0}{R^2} \left[\frac{m_P}{m_e}\right]^{1/2} \frac{n_0^2 A_0 L_0^2}{T_0^2} \left[\frac{T_0}{\varepsilon}\right]^4 e^{-\varepsilon/T_0} \left(2 + \frac{2\varepsilon}{T_0} + \frac{\varepsilon^2}{T_0^2}\right) \qquad (33)$$

for the complete Maxwellian, and

$$\mathscr{I}_b(\varepsilon)=\frac{3}{(2\pi)^{3/2}}\frac{\sigma_0}{R^2}\left[\frac{m_P}{m_e}\right]^{1/2}\frac{n_0^2A_0L_0^2}{T_0^2}\left(\frac{T_0}{\varepsilon}\right)^4\times$$

$$\times\begin{cases}\left[e^{-\varepsilon/T_0}\left(2+\dfrac{2\varepsilon}{T_0}+\dfrac{\varepsilon^2}{T_0^2}\right)+\frac{1}{3}e^{-\alpha}\left(\dfrac{\varepsilon}{T_0}\right)^3\right] & \varepsilon\le\alpha T_0\\ -e^{-\alpha}\left(2+\dfrac{2\varepsilon}{T_0}+\dfrac{\varepsilon^2}{T_0^2}\right)-\frac{1}{3}e^{-\alpha}\alpha^3 & \\ 0\quad\ldots\qquad\varepsilon>\alpha T_0 & \end{cases} \tag{34}$$

for the truncated Maxwellian, where we have set $\alpha=\frac{1}{2}(m_P/m_e)^{1/4}\simeq 3.38$ and $t_0=\frac{2}{3}L_0/(T_0/m_p)^{1/2}$.

To evaluate the thick-target emission from the tail we assume purely collisional energy losses of the form $\mathrm{d}E/\mathrm{d}t=-K'n_pv/E$, where n_p is the plasma density along the electron path and K' is approximately constant. Then, following Brown (1971), the pulse of thick-target X-rays emitted by *one* tail electron of initial energy E_0 can be expressed as follows:

$$\Delta\mathscr{I}_t(\varepsilon,E_0)=\frac{1}{4\pi R^2}\int_t n_pv\frac{\sigma_0}{\varepsilon E}\,\mathrm{d}t=\frac{1}{4\pi R^2}\int_{E=\varepsilon}^{E_0}\frac{n_pv\sigma_0}{\varepsilon E}\frac{\mathrm{d}E}{(K'n_pv/E)}=$$

$$=\frac{\sigma_0}{4\pi R^2K'}\left(\frac{E_0}{\varepsilon}-1\right)\text{ (photons cm}^{-2}\text{ per unit }\varepsilon). \tag{35}$$

The number of electrons escaping from the kernel per unit E_0 is

$$N(E_0)=\begin{cases}\dfrac{2}{\pi^{1/2}}n_oA_0L_0\dfrac{E_0^{1/2}}{T_0^{3/2}}e^{-E_0/T_0} & E_0\ge\alpha T_0\\ 0 & E_0<\alpha T_0\end{cases} \tag{36}$$

so the total thick-target pulse emitted has a spectrum

$$\mathscr{I}_t(\varepsilon)=\int_{\max(\varepsilon,\alpha T_0)}^{\infty}N(E_0)\Delta\mathscr{I}_t(\varepsilon,E_0)\,\mathrm{d}E_0=$$

$$=\frac{1}{2\pi^{3/2}}\frac{\sigma_0}{R^2}\frac{n_0A_0L_0}{K'}\times$$

$$\times\begin{cases}\left(\dfrac{T_0}{\varepsilon}\right)\alpha^{3/2}e^{-\alpha}+\left(\dfrac{3}{2}\dfrac{T_0}{\varepsilon}-1\right)\Gamma(\alpha,\frac{3}{2}) & \varepsilon\le\alpha T_0\\ \left(\dfrac{\varepsilon}{T_0}\right)^{1/2}e^{-\varepsilon/T_0}+\left(\dfrac{3}{2}\dfrac{T_0}{\varepsilon}-1\right)\Gamma(\varepsilon/T_0,\frac{3}{2}) & \varepsilon>\alpha T_0\,.\end{cases} \tag{37}$$

Thus, the spectrum from a truncated Maxwellian kernel plus tail deposited in a

thick-target, in the upper-limit case, is

$$\mathscr{I}_c(\varepsilon) = \mathscr{I}_b(\varepsilon) + \mathscr{I}_t(\varepsilon)\,. \tag{38}$$

We note that the tail contribution is related to the thermal contribution by

$$\frac{\mathscr{I}_t}{\mathscr{I}_b} = \frac{2^{1/2}}{3}\left[\frac{m_e}{m_p}\right]^{1/2} \frac{T_0^2}{n_0 L_0 K'} F(\varepsilon/T_0) \simeq \frac{10^{-2}}{\Delta} F(\varepsilon/T_0)\,, \tag{39}$$

where F is a dimensionless function ($\to\infty$ at $\varepsilon > \alpha T_0$) and

$$\Delta = n_0 L_0 \frac{K'}{T_0^2} \simeq 10^{-3} \frac{n_0 \cdot (10^{11}\ \mathrm{cm}^{-3}) L_0(\mathrm{km})}{T_0^2\ (\mathrm{keV})} \tag{40}$$

is the ratio of the kernel length L_0 to the collisional mean free path l_c of a thermal electron, or a measure of how collisionally thick the kernel is. The parameter Δ is constrained to be $\lesssim 1$ by the basic requirements for sustaining an ion-acoustic conduction front throughout the kernel decay. If Δ were large, collisions would prevent the electron streaming necessary to generate an unstable reverse current, thereby prohibiting the continuous production of the conduction front. More specifically, if the heating results in a kernel of size L separated from cool surroundings by a layer of thickness l which increases as the kernel cools, then ion-sound wave generation will be sustained only as long as $l \lesssim l_c$ – i.e. for a time $\ll L/v_s$ unless $\Delta \lesssim 1$. In any case it is clear from (40) that Δ is small for plausible densities and temperatures, and for sizes consistent with our previous considerations.

In Figure 2 we show the resultant kernel spectra $\mathscr{I}(\varepsilon)$ for the three cases (a), (b), and (c) for two values of Δ. For $\Delta \geq 10^{-1}$ the contribution to $\mathscr{I}(\varepsilon)$ from the escaping tail is only important at high energies. For $L_0 \lesssim 10^3$ km and $n_0 \lesssim 10^{11}$ cm^{-3}, however, Δ could be small enough for the tail contribution to dominate even at $\varepsilon \simeq T_0$. This is an alternative expression of the fact, already noted by BMS and by Smith and Lilliequist (1979), that thermal bremsstrahlung sources are only more efficient than non-thermal sources for sufficiently high densities. In actual solar-flare conditions this tail contribution is likely to fall well below our upper-limit estimate, due to the non-collisional energy losses already mentioned. Unfortunately, no adequate treatment incorporating these losses exists as yet.

5. Discussion and Conclusions

Our main contention is that any dissipative thermal interpretation of hard X-ray bursts (even in the case of single spike bursts) should be based not on a *single* hot source of lifetime comparable to the burst duration, but rather on the continuous production of many short-lived hot kernels throughout the burst. This proposal initially was based on the fact that a single, conductively-cooled kernel at constant density (cf. Section 2) cannot reproduce the observed fall of total source emission measure with temperature during burst decay; a suitable rate of kernel production, on the other hand, *could* produce this behaviour. The numerical results of Smith and

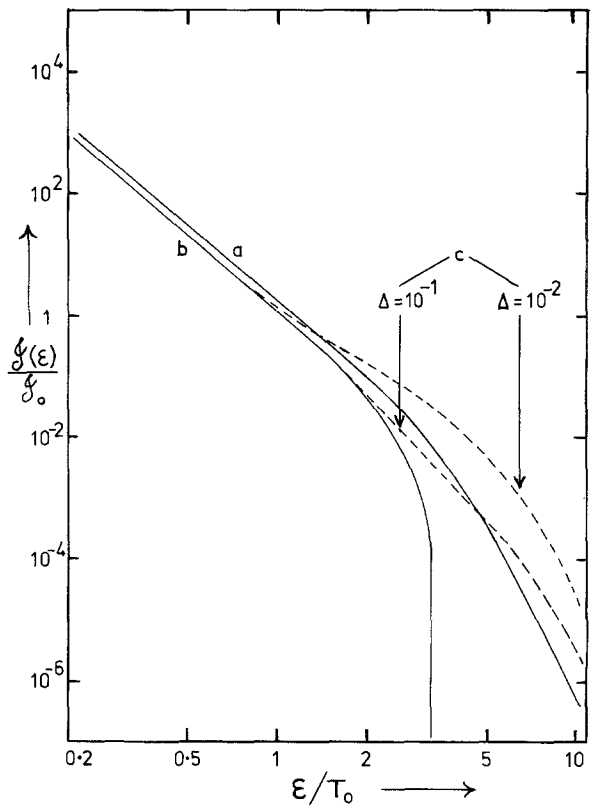

Fig. 2. Spectrum $\mathcal{I}(\varepsilon)$ emitted during lifetime of a 1-D BMS kernel under three limiting conditions: (a) kernel electrons having a complete Maxwellian distribution at temperature T_0; (b) kernel electron distribution being a Maxwellian truncated at $E = \alpha T_0$; (c) electron distribution as in (b) but with the additional contribution of an electron tail above $E = \alpha T_0$ escaping to a collisional thick target. In case (c) Δ measures the collisional thickness of the thermal kernel. In all cases $\mathcal{I}(\varepsilon)$ is expressed relative to $\mathcal{I}_0 = 3/(2\pi)^{3/2} \times (m_p/m_e)^{1/2} \times \sigma_0 n_0^2 A L_0^2/(R^2 T_0^2)$.

Lilliequist (1979) and of Auer and Smith (1979), however, do exhibit significant density changes due to hydrodynamic effect on electron-conduction time scales, despite the fact that $T_e \gg T_p$. It is not clear at this stage why their results differ from those of BMS in this respect, though their use of a continuous, rather than an impulsive, heat input may provide a partial explanation. Furthermore, their artificial adoption of a heating function per unit volume fixed in space rather than moving with the gas certainly will exaggerate any density decrease once started (due to the unrealistic increase in heating per unit mass). In any case, if expansion effects do prove important it may not be essential to invoke any dynamic kernel model to explain the observed $EM(t)$ versus $T(t)$ behaviour.

There are independent reasons, however, for believing that dynamic kernel production is the most appropriate model of solar-flare source structure. On theoretical grounds, the most efficient mechanisms for magnetic energy dissipation

(e.g. the double tearing mode) involve field annihilation at many points throughout the energy storage region. Ideally, therefore, we should like to see development of the analysis of such modes to the point where it is possible to put some bounds on the kernel source function $Q(T_0, EM_0, t_0)$, which appears in Equation (9) (cf. Spicer, 1976; van Hoven, 1979). A second consideration is that spectral-line density diagnostics lead to paradoxes which are most likely resolved in terms of a transient ionisation equilibrium state existing in a series of kernels in a dynamic dissipation situation (see Brown and Nakagawa, 1978; and references therein). Therefore, while concentrating on the BMS conductively-cooled kernel model, we have formulated our analysis so that it could be extended to other situations, such as those where density changes are important, by evaluation of the appropriate $\mathscr{I}_K(\varepsilon)$ from Equation (3).

We conclude that the hardest burst spectra observed can be reconciled with the model only if 3-D conduction, or a more general conduction law than that considered by BMS, is involved. We point out also that the X-ray spectrum at higher energies may be crucially determined by the as yet uncertain characteristics of the electron tail. As far as other flare observations are concerned, a dynamic kernel situation will be even more complex to analyse than the BMS case of a single hot kernel, in terms of microwave emission from the electron tail and in terms of chromospheric response to the hot conduction fronts. The dynamic model may lead to smaller X-ray polarisations than the estimates made for a single conductive kernel model by Emslie and Brown (1979), due to complex geometry of kernel distribution.

One final aspect of the problem which must be considered is the effect of dynamic kernel production, as opposed to a single-kernel source, on the energetic requirements for thermal bremsstrahlung. This can be assessed by considering the thermal energy input $\mathscr{E}$ required to produce a burst yielding $\mathscr{I}_B$ photons cm^{-2} per unit ε at the Earth over a burst duration t_x. For simplicity, we consider only $\varepsilon \simeq T_0$, and the 1-D BMS kernel. According to Equation (8), the photon yield from one kernel is

$$\mathscr{I}(\varepsilon \simeq T_0) = \frac{15C}{2e} \frac{n_0^2 A L_0 t_0}{T_0^{3/2}}, \tag{41}$$

where e is exponential e. Since each kernel has a thermal energy $\Delta\mathscr{E} \simeq \frac{3}{2} n_0 A L_0 T_0$, the total thermal energy release required is

$$\mathscr{E} = \frac{\mathscr{I}_B}{\mathscr{I}} \Delta\mathscr{E} = \frac{e\mathscr{I}_B}{5C} \frac{T_0^{5/2}}{n_0 t_0} = \frac{e\mathscr{I}_B}{5Cm_P^{1/2}} \frac{T_0^3}{n_0 L_0}. \tag{42}$$

In the case of a single thermal source producing the complete burst spike, $t_0 \equiv t_x$ and L_0 is therefore fixed (cf. BMS). For the dynamic model, on the other hand, $t_0 \ll t_x$ and we see that *for a fixed* n_0 the dynamic kernel model requires more energy dissipation than the single kernel by the factor t_x/t_0, that is, proportional to the number of kernels present. Physically this is because the conduction lifetime of each kernel is smaller for smaller sizes L_0. A similar conclusion can be drawn readily for the 3-D case. Consequently, the energy supply (or efficiency) advantage of thermal over

nonthermal models can be retained in a dynamic kernel situation only by adoption of appropriately higher source densities n_0. An increase in n_0 will not violate the condition $\Delta \ll 1$ required for maintenance of anomalous conduction (see Equation (40) and subsequent discussion) since it is accompanied by a proportionate decrease in L_0. However, n_0 clearly cannot be increased arbitrarily without violating other observational and theoretical constraints (e.g. Brown and Nakagawa, 1978), and it is necessary to steer a careful path in the choice of parameters if the thermal model is to maintain its efficiency advantage.

Acknowledgements

This work has benefited from discussion with D. S. Spicer, P. Hoyng, A. Duijveman, and D. F. Smith. The authors wish to acknowledge the support of a UK Science Research Council Grant (J.C.B and I.J.D.C.) and NASA grant NSG 033 (J.T.K).

References

Acton, L. W.: 1968, *Astrophys. J.* **152**, 305.
Arnoldy, R. L., Kane, S. R., and Winckler, J. R.: 1968, *Astrophys. J.* **151**, 711.
Auer, L. and Smith, D. F.: 1979, preprint.
Brown, J. C.: 1971, *Solar Phys.* **18**, 489.
Brown, J. C.: 1974, in G. A. Newkirk (ed.), 'Coronal Disturbances', *IAU Symp.* **57**, 395.
Brown, J. C.: 1978, *Astrophys. J.* **225**, 1076.
Brown, J. C. and Nakagawa, Y.: 1978, *Astrophys. J.* **225**, L153.
Brown, J. C., Melrose, D. B., and Spicer, D. S.: 1979, *Astrophys. J.* **228**, 592.
Chubb, T. A.: 1970, in E. R. Dyer (ed.), *Solar Terrestrial Physics*, Part 1, D. Reidel Publ. Co., Dordrecht, Holland, p. 99.
Colgate, S. A.: 1978, *Astrophys. J.* **221**, 1068.
Craig, I. J. D. and Brown, J. C.: 1976, *Astron. Astrophys.* **49**, 239.
Craig, I. J. D., McClymont, A. N., and Underwood, J. H.: 1978, *Astron. Astrophys.* **70**, 1.
Crannell, C. J., Frost, K. J., Mätzler, C., Ohki, K., and Saba, J. L.: 1978, *Astrophys. J.* **223**, 620.
Datlowe, D. W., Hudson, H. S., and Peterson, L. E.: 1974a, *Solar Phys.* **35**, 193.
Datlowe, D. W., Elcan, M. J., and Hudson, H. S.: 1974b, *Solar Phys.* **39**, 155.
Drake, J. F. and Lee, Y. C.: 1977, *Phys. Fluids* **20**, 1341.
Duijveman, A. and Hoyng, P.: 1980, preprint.
Elcan, M. J.: 1978, *Astrophys. J. Letters* **226**, L99.
Emslie, A. G. and Brown, J. C.: 1980, *Astrophys. J.*, in press.
Fürth, H. P., Killeen, J., and Rosenbluth, M. N.: 1963, *Phys. Fluids* **6**, 459.
Hoyng, P., Brown, J. C., and van Beek, H. F.: 1976, *Solar Phys.* **48**, 197.
Ionson, J.: 1978, paper presented at *AAS Meeting on the Solar Maximum Mission*, Ann Arbor, November, 1978.
Kahler, S.W.: 1971a, *Astrophys. J.* **164**, 365.
Kahler, S. W.: 1971b, *Astrophys. J.* **168**, 319.
Kahler, S. W.: 1975, in S. R. Kane (ed.), 'Solar Gamma-, X-, and EUV Radiation', *IAU Symp.* **68**, 211.
Kane, S. R.: 1974, in G. A. Newkirk (ed.), 'Coronal Disturbances', *IAU Symp.* **57**, 105.
Kane, S. R. and Anderson, K. A.: 1970, *Astrophys. J.* **162**, 1003.
Karpen, J. T., Crannell, C. J., and Frost, K. J.: 1979, *Astrophys. J.*, in press.
Mätzler, C., Bai, T., Crannell, C. J., and Frost, K. J.: 1978, *Astrophys. J.* **223**, 1058.
Smith, D. F. and Brown, J. C.: 1979, preprint.
Smith, D. F. and Lilliequist, C. G.: 1979, *Astrophys. J.* **232**, 582.

Spicer, D. S.: 1976, U.S. NRL Report No. 8036.
Spicer, D. S.: 1977, *Solar Phys.* **53**, 305.
van Hoven, G.: 1979, *Astrophys. J.* **232**, 572.
Vlahos, L. and Emslie, A. G.: 1979, in preparation.
Vlahos, L. and Papadopoulos, D.: 1979, *Astrophys. J.* **233**, 000.
Zaumen, W. T. and Acton, L. W.: 1974, *Solar Phys.* **36**, 139.
Zeldovich, Ya. B. and Raizer, Yu. P.: 1967, *Physics of Shock Waves and High Temperature Hydrodynamic Phenomena*, Academic Press.